Industrial Crops & Products 220 (2024) 119233

Contents lists available at ScienceDirect

Industrial Crops & Products

journal homepage: www.elsevier.com/locate/indcrop

Convolutional neural networks to assess bergamot essential oil content in the field from smartphone images

Matteo Anello [a,1], Fernando Mateo [b,1], Bruno Bernardi [a,*], Angelo Maria Giuffrè [a], Jose Blasco [c], Juan Gómez-Sanchis [b]

[a] Dipartimento di Agraria, Università Mediterranea di Reggio Calabria, Reggio Calabria, Italy
[b] Department of Electronic Engineering, University of Valencia, Valencia, Spain
[c] Centro de Agroingeniería, Instituto Valenciano de Investigaciones Agrarias (IVIA), Carretera CV-315, Km 10.7, Moncada 46113, Spain

ARTICLE INFO

Keywords:
Cv. Fantastico
Cv. Femminello
Smartphone camera
Essential oil
Deep learning

ABSTRACT

The essential oil (EO) extracted from bergamot peel (*Citrus bergamia*, Risso et Poiteau) is appreciated in perfumery and gastronomy. Notably, 90 % of the bergamot EO production is concentrated in the Province of Reggio Calabria (Southern Italy) under a protected designation of origin (PDO). The early estimation of EO content in fruits is fundamental to help farmers in their decision at harvesting period. The application of advanced modelling techniques based on artificial intelligence and digital device technology can contribute to this goal. This study proposes a method to estimate the EO content of fruits in the field using classification and regression models based on a deep learning approach in two cultivars: cv. "Fantastico" and cv. "Femminello". The first step was to capture images of the fruit in the Red, Green, and Blue colours (RGB) using a mid-range smartphone camera and a portable inspection chamber designed and developed for this study. The acquisition of the images was carried out in the field. The fruits were collected and transported to the laboratory, where the EO was extracted using steam hydrodistillation. Custom-built convolutional neural networks (CNN) and three transfer learning models (VGG-16, VGG-19, and Xception architectures) were trained and applied for classification (among different discrete levels of oil content) and regression (to predict the EO content). The classification results showed an accuracy of 0.795 and 0.797 on the test samples of the two cultivars separately, while the best regression model achieved a minimum mean squared error of 0.12 and 0.04 for each cultivar, respectively. The results showed the effectiveness of the approach tested and how modelling each variety independently can lead to better performance for the CNNs tested.

1. Introduction

Bergamot (*Citrus bergamia,* Risso et Poiteau) is an evergreen plant of great interest for the appreciated essential oil (EO) contained in the flavedo and for its juice, which is rich in antioxidants (Di Donna et al., 2020; Giuffrè., 2019). The principal cultivation area is a narrow coastal strip of approximately 150 km in Reggio Calabria Province (Southern Italy). Notably, 90 % of EO is produced in this area (Amato et al., 2013), protected under the designation of origin (PDO) Bergamot of Reggio Calabria (Benalia et al., 2023). Bergamot is appreciated in perfumery and cosmetics for its intense fragrance and freshness (Gioffrè et al., 2020), is considered the green gold of all master perfumers, and has become an essential ingredient in the most prestigious perfumes worldwide (Dugo and Bonaccorsi, 2013). From an economic perspective, 95 % of the bergamot EO is exported, predominantly to France, England, Germany, the USA, Japan, India, Australia, and China. Bergamot is the second main product of the Italian citrus industry (Fatta Del Bosco et al., 2020). However, due to its EO content, it is the most expensive in comparison to lemons, mandarins, clementines and oranges (Patrizia Capua., 2015).

The most important cultivars are cv. "Fantastico" and cv. "Femminello". These cultivars differ mainly in the appearance of the fruit: cv Femminello has a small and smooth fruit and is the most productive; cv Fantastico produce more elongated fruits, resembling a pear. Harvesting

* Corresponding author.
E-mail addresses: matteo.anello@unirc.it (M. Anello), fernando.mateo@uv.es (F. Mateo), bruno.bernardi@unirc.it (B. Bernardi), amgiuffre@unirc.it (A.M. Giuffrè), blasco_josiva@gva.es (J. Blasco), juan.gomez-sanchis@uv.es (J. Gómez-Sanchis).
[1] These authors contributed equally to the work.

https://doi.org/10.1016/j.indcrop.2024.119233
Received 12 August 2023; Received in revised form 13 July 2024; Accepted 14 July 2024
Available online 18 July 2024

takes place between November and December when the fruit reaches its maximum oil content. The peel is up to 6 mm thick, characterised by a shiny green colour at the beginning of the productive season, and turns pale yellow when the fruit is ripe, which indicates its maturity. Yellow-ripe fruits are used to extract EO, whereas unripe green fruits are used mainly in the confectionery industry (Consorzio di tutela del bergamotto., 2023). The amount of fruit harvested ranges approximately between 15,000 and 20,000 tonnes per year, producing around 80–100 thousand kilos of EO. The peel contains several glands enclosing the EO (Quirino et al., 2022), which present a greenish colour at the beginning of the productive season and turn brownish yellow at the end (Navarra et al., 2015). EO is obtained mainly from plant materials by steam distillation, by mechanical processes from citrus epicarp, or by dry distillation after separation of the aqueous phase, if any, by physical processes (International Organization for Standardization ISO., 2013).

The early estimation of EO is fundamental to identifying the optimal ripening stage according to colour. Hunter (2010) reported that unripe fruits are easier to squeeze because the force required to release the EO is inversely proportional to the ripeness index. The optimum harvesting time to optimise the EO extraction has traditionally been determined by visual assessment of fruit colour. This condition requires the great experience of the grower, but it is based on strict personal judgement and, hence, subjective. An alternative could be the use of technology to obtain and analyse fruit images to objectively determine skin colour and make informed decisions regarding the best harvesting moment. Different sensors can acquire images in the field, such as thermal (Cohen et al., 2022), multi-or hyperspectral (Munera et al., 2021), stereo (Lohar et al., 2021), and colour (Gonzalez-Gonzalez et al., 2021) cameras. Colour cameras are the most appropriate for price, simplicity, and similarity to human perception.

Another challenge in agriculture is monitoring fruit quality parameters in the field (Sola-Guirado et al., 2020). Today, smartphones are useful and affordable with high-quality, high-resolution cameras and powerful computing capabilities (Blahnik and Schindelbeck, 2021). Their main advantage is accessibility; almost all farmers have devices in their pockets. Therefore, there is a trend toward developing new field applications for these devices (Wang et al., 2018). An example is an application developed by Cubero-García et al., (2018) using smartphones to determine the colour citrus index (CCI) of oranges and mandarins in the field, to realise its measure automatically.

The information captured by cameras must be analysed to obtain accurate and repeatable results. Artificial intelligence (AI) has recently emerged as a powerful technique for emulating the human visual system to interpret and classify image content (Elgendy, 2020). A broad area of AI is closely related to image classification in agriculture, where enormous progress has been made in many domains, including pest and disease classification, fruit recognition, precision agriculture and decision support systems (Kujawa and Niedbała, 2021; Fazari et al., 2021; Jia et al., 2020; Kamilaris and Prenafeta-Boldú, 2018; Teke et al., 2013; Benalia et al., 2015). Image classification is strictly related to Convolutional Neural Networks (CNNs), a class of Artificial Neural Networks (ANNs) generally intended to perform visual analysis on computers (Carnagie et al., 2022). According to Fajardo Muñoz et al. (2023) and El-Attar et al. (2020), CNNs can contribute to solve several issues related to biological compounds extracted from different parts of aromatic plants, such as flowers and leaves, and predict the EO extraction yield. Carnagie et al. (2022) proposed a custom CNN network to perform image recognition and classification of ten major plant species capable of producing useful EOs, one of the most important being bergamot.

However, no previous studies have estimated the EO content of citrus peels using automated and non-destructive field sensors. This research aims to test the potential of CNNs for (i) classification and (ii) prediction of the amount of EO using a specific tool to acquire fruit images in the field.

2. Material and methods

2.1. Field sampling

Two bergamot plantations with trees of cv Fantastico and cv Femminello, aged 15–20 years, were studied. The two research areas were located at 37°58'49"N 16°05'25"E and 38°01′56″N 15°39′47″E, respectively. Tests were conducted on flat terrain, on average 20-meter asl, under similar weather conditions, with trees in health. The rootstocks used were bitter orange (*Citrus aurantium* L.) for cv Fantastico and Citrange Troyer (*Poncirus trifoliata* (L.) Rat. × *Citrus sinensis* (L.) Osbecke). The soil contained 23 % (by volume) of rock fragments larger than 2 mm in diameter. The texture comprised 26.4 % sand, 42.1 % silt, and 31.5 % clay. The concentration of organic matter in the soil was 5.1 %, pH 8, and the total calcium ($CaCO_3$) was 4 %. The average monthly temperature was 19 °C, and the monthly rainfall was 49.5 mm.

Mineral fertilisation (1 kg/plant) was carried out using a ternary fertiliser (11 N–22 P_2O_5 - 16 K_2O), fertigation by potassium nitrate (2500 kg/ha twice a year), and foliar fertilisation with algae extracts and boron. Between May and October, 80 L of water was provided to each plant twice a week. Phytosanitary management includes uprooting in the event of Mal Secco disease. The Bayer Movento 48SC insecticide was used twice a year in early and late spring to control sucking pests (aphids, leaf miners, and mealybugs) at a dose of 200 g/100 L of water. Mowing was realised three times a year. On average, the production yield of the fresh product was approximately 35 tonnes/ha, whereas that of the EO was 16 kg/ha.

Sampling was carried out by taking 100 images of bergamot fruit on nine dates, from 03 November 2022–04 January 2023. Fruits were chosen according to the ripening evolution evaluated by the Citrus Colour Index (CCI) defined by Jiménez-Cuesta et al. (1981) using the standard Citrus Colour Chart developed by the Valencian Institute of Agricultural Research (IVIA). This index is applied in the citrus industry to assess fruit colour and determine the optimal harvesting period, obtained using a standard citrus colour chart. The sampling fruit had the same CCI values. Five CCI values (−9, −5, −3, +1, and +3) were established according to the PDO specifications, which reported that the fruit must be harvested when the colour ranges from green to yellow.

The previous year, sampling was carried out on the only cv Fantastico on four dates: from 02/12/2021 to 20/01/2022, as a reference to verify the setting. Three CCI values were recorded (−5, −3, and +3). All the dates of sampling and the CCI values are summarised in Table 1.

Images were captured using a smartphone (Huawei P9 Lite) with 3 GB RAM (Kirin 650); the main features of the smartphone are listed in Table 2.

A low-cost portable inspection chamber was constructed to prevent interference from natural light during image acquisition. The inspection

Table 1
Sampling dates and CCI value for cv Fantastico and cv Femminello.

Date	CCI	CCI
(2022/2023)	Fantastico	Femminello
03/11/2022	-9	-9
10/11/2022	-9	-5
17/11/2022	-5	-5
24/11/2022	-5	-3
01/12/2022	-3	1
06/12/2022	-3	3
15/12/2022	1	3
20/12/2022	3	3
04/01/2023	3	3
Date	CCI	
(2021/2022)	Fantastico	
02/12/2021	-5	
16/12/2021	-3	
04/01/2022	+3	
20/01/2022	+3	

Table 2
Detailed parameters of the smartphone.

Parameter	Description
CPU	HiSilicon Kirin 650
GPU	Mali-T830MP2
RAM	3 GB Kirin 650
Cameras	13 MP
Operating System	Android 6.0

chamber consisted of a black plastic tube containing a diffuse light-emitting diode (LED) ring light (6500 K), allowing the maintenance of image acquisition under controlled conditions (Fig. 1). For each fruit, four images were acquired to capture the colour variations, for a total of 400 images per sampling date.

First, the CCI was calculated using a portable spectrophotometer (CM-700d, Konica Minolta, Tokyo, Japan) to optimise the accuracy of colour acquisition by the mobile camera. Images acquired by the mobile camera, set with different configurations, were analysed using Food Colour Inspector software, a tool developed at the Laboratory of Artificial Vision of IVIA (Spain). The linear regression between the CCI values obtained from the image of the mobile camera and the handheld spectrophotometer gave a coefficient of determination R^2 of 0.93, which was considered acceptable. Based on this outcome, the mobile camera was set with the following acquisition parameters: F-stop f/2, exposure time of 1/200 s, and ISO 100 (Anello et al., 2023). The images were stored in JPEG format.

2.2. EO extraction

After image acquisition, fruits were randomly collected by hand and transported to the laboratory for EO extraction by hydrodistillation. The bergamot peel was carefully removed with a knife and crushed to reduce size. Crushed pieces of bergamot peel (250 g) were placed into a 2000 ml round bottom flask and 1000 ml of distilled water was added to it. The flask was heated to a boiling point and held for 2 h. The vapour mixture was then condensed and distilled in the Clevenger apparatus, and the EO was recovered and quantified in grams. This procedure was repeated twice for each extraction performed.

2.3. Convolutional neural networks architecture

CNNs were built and trained for two different tasks:

1. *Classification task*: CNNs were used to estimate the EO content by classifying it into discrete classes. In this approach, the continuous variable representing EO content was discretised into classes and the goal was to assign each instance to one of the discrete classes. This classification problem was approached in two different ways:

a. Two models to classify EO discrete levels of each cultivar. These classifiers tried to classify the EO level of the fruits of each cultivar independently (9 classes for cv Fantastico and 5 for cv Femminello);
b. One general model to classify EO discrete levels of both cultivars. This classifier attempts to determine one of the cultivar/EO discrete level combinations (8 classes spaced 19 grammes between each other).

2. *Regression or function approximation task:* CNNs were employed to estimate the EO content as a continuous variable. In this case, the model aims to predict the exact numerical value of the EO content rather than assigning it to discrete classes. This task involves regression or function approximation, where the network learns to predict a continuous output. This regression approach was also addressed using:

a. Two models to estimate the EO content for each cultivar independently;
b. One general model to estimate EO the content for both cultivars jointly.

In principle, EO content is a numerical variable and a regression approximation is more appropriate, but in this scenario, there are few different values of EO and many images assigned to the same EO value. This fact could prove that images belonging to distinct clusters or groups

Fig. 1. Portable inspection chamber. a) Overall view; b) Field use; c) Graphical representation d) In-room lighting system.

of samples with different EO content levels may have similar patterns (feature maps). In this kind of scenario, a classification approach can be effective in capturing these patterns.

2.3.1. Datasets implemented

The dataset was created considering the values of EO content. The EO content is influenced by various factors such as genetics, climate, soil conditions, and the maturity of the fruit. However, there is a correlation between colour and EO content due to factors like maturity (more mature fruits might have higher oil content), and growers use this relationship to determine the harvesting moment visually. EO content is somehow related to the maturity stage and, hence, the colour. Moreover, The CNNs used to process the image are deep learning algorithms that can capture hidden relationships and other image features different from colour, such as the texture, which can also be related to the EO content. Hence, the class labels were set as shown in Tables 3, 4 and 5. The R, G, and B coordinates of the pixels belonging to the fruit were used as inputs to the models.

2.3.2. Pre-processing

Before the creation of the predictive models, a pre-processing stage was performed on the input images to correct possible acquisition errors, noise, or deviations in the pixel values and to adapt them to the learning models so that they could learn optimally.

2.3.2.1. Image rescaling. The first pre-processing step was applied to rescale the three channels of all images between zero and one. This helps to uniformise the possible uneven brightness levels of the different images so that this difference in pixel range is not used as a feature to minimise the loss of the model during the training stage. Because the RGB images are coded with 8 bits/pixel in each channel (representing a pixel value range in [0255]), the normalisation of each channel (c_R, c_G, c_B) is

$$c_i' = \frac{c_i}{255}, \quad i = R, G, B$$

2.3.2.2. Image resizing. Another pre-processing step was to resize the images from the original 4160 × 3120 or 3120 × 4160 pixels to a unique size. This was necessary to ensure that all input image sizes were used as input features for the developed models. The original high-resolution images contained fine detail, irrelevant to the prediction goal. Reducing the images shorted training times without a reduction in performance.

First, the images were squared to fit the 2D convolutions with squared filters. Second, as one of the goals of this work was to use transfer learning techniques to predict oil content, the transfer learning models used were pre-trained with the ImageNet dataset (Deng et al., 2009), which was adapted to a standard ImageNet size of 224 × 224 pixels. This approach has often been adopted in the literature for optimal compatibility (Paymode and Malode, 2022). An example of an image obtained after the pre-processing stage is shown in Fig. 2.

Table 3
Oil content (± standard deviation) and the class labels for cv Fantastico.

Oil content (g)	Class label
2.87 ± 0.18	0
3.45 ± 0.19	1
3.56 ± 0.02	2
3.88 ± 0.39	3
4.02 ± 0.30	4
4.16 ± 0.10	5
4.52 ± 0.17	6
4.76 ± 0.09	7
5.00 ± 0.18	8

Table 4
Oil content (± standard deviation) and the class labels for cv Femminello.

Oil content (g)	Class label
3.38 ± 0.17	0
3.58 ± 0.21	1
3.66 ± 0.08	2
3.94 ± 0.22	3
4.16 ± 0.07	4

Table 5
Oil content and the class labels for the general model.

Oil content (g)	Class label
≤ 3.30	0
3.31–3.50	1
0.51–3.70	2
3.71–3.90	3
3.91–4.10	4
4.11–4.30	5
4.31–4.55	6
≥ 4.56	7

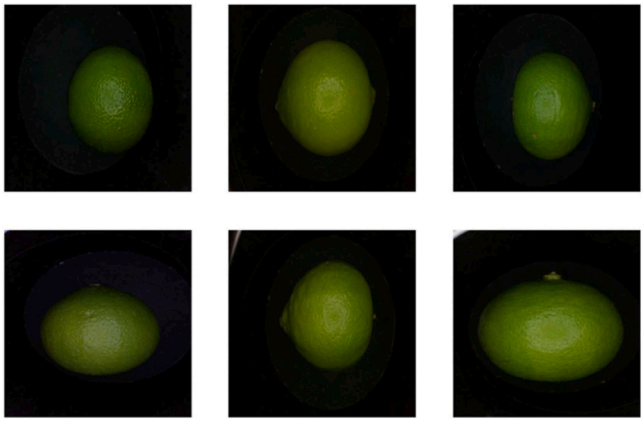

Fig. 2. Example of six bergamot fruit images after the pre-processing stages.

2.3.2.3. One-hot encoding of outputs. When using classification models, the label values must also be processed to remove the cardinality effect (i.e. relative distances between class representations which could encode some artificial ordering); this is because, in our models, we had one output node per label, each with a softmax activation function that produced probability levels between 0 and 1. Therefore, the output for each image in the sample is a vector composed of as many elements as classes, following a "one-hot" representation. In this type of representation, only one of the elements of the vector is 1 (the index corresponding to the class value), while all other elements are set to zero. Every time a prediction for a sample was obtained from the CNN, the Argmax function was applied to the outputs to determine the predicted class index.

2.3.3. Training and validation datasets

TensorFlow/Keras Python libraries were used for model development. In these libraries, the training data enable the model to learn by adjusting its weights iteratively, whereas the validation data are used to assess the generalisation on an external dataset after each weight adjustment. The approach consisted of training for a maximum of 100 epochs until the validation error reached a plateau and did not improve further. An early stopping procedure was implemented to avoid overfitting, and the training process was stopped if the validation loss did not improve for 10 consecutive epochs. After training, the best model

weights (those that produced the lowest cross-entropy loss in the validation set history) were saved using the Keras model checkpoint function. Finally, the model is evaluated using a test set for an unbiased accuracy estimation.

To correctly assess the model generalisation capabilities, the captured images were randomly split into training (60 %), validation (20 %), and test (20 %) sets. All the classes were equally distributed among the three groups. Depending on the approach, the final tensor sizes used to create the models are listed in Table 6.

2.3.4. Models

2.3.4.1. Custom classifier. The first approach is to create a classifier (or two classifiers for the second classification approach) to estimate the EO discrete levels encoded as the target classes. A custom CNN model was created from scratch, and its performance was compared with that of the other pre-trained classifiers using *transfer learning* for fine-tuning.

The architecture followed the same principles as the VGG CNN architectures but with lower complexity. It comprises three functional blocks with (i) two consecutive 2D convolution layers that added depth to the feature maps, both using 3 × 3-pixel filters and "same" padding to avoid reducing the feature map width and height and (ii) a max pooling layer with 2 × 2 filters with stride = 2, that kept the maximum value from each 2 × 2-pixel window in the feature map, thus halving the width and height of the feature map at each step. The top of the CNN comprised a flattened layer and a fully connected structure with 128 hidden nodes with ReLU activation, a dropout layer with probability p = 0.2, and nine output nodes with softmax activation that provided the class probabilities. The custom CNN model architecture proposed for the general classifier is shown in Supplementary Figure 1, including input/output tensor sizes for each block. The same architecture was used for separate classifiers with a difference in the number of outputs in the last dense layer (9 or 5 instead of 8).

2.3.4.2. Transfer learning models. In the present work, VGG-16, VGG-19 (Simonyan and Zisserman, 2014), and Xception (Chollet, 2017) model architectures were used as starting points to build the transfer learning models. In each layer, the top layers were removed and replaced by a block that produced the mapping from the original feature map depth of 512 (for VGG-16/19) or 2048 (for Xception) to only 8 outputs (in the general model), representing our model classes. The new top layers are made of fully connected structures composed of a flattening layer, two dense layers with 1024 and 512 neurones, respectively, with ReLU activation functions and dropout layers with a dropout probability of 0.3 to help reduce overfitting and an output layer of as many nodes as classes with softmax activations. The resulting architectures for the general model, including the input and output tensor sizes for each block, are shown in Supplementary Figure 2. For the separate models, the only difference was in the number of outputs in the last dense layer. The models were trained for a maximum of 100 epochs in batches of 64 samples using the Adam optimiser and minimising cross-entropy loss.

2.3.4.3. Regression models. For the regression approach, we implemented a model derived from a custom classifier, replacing the last fully connected part with a single layer of 128 nodes and ReLU activation, followed by a single node with linear activation to yield a real value. The architecture is shown in Supplementary Figure 3. The same preprocessing and dataset splitting were performed for classification (Table 3), except that the target variable was a real number (EO content in grams), and the loss function was the minimisation of mean squared error (MSE) between the target and the predicted value. We trained the models for a maximum of 100 epochs, implementing the same early stopping procedure and using a batch size of 64, similar to that in the classification approach.

Table 6
Tensor sizes for training, validation and test subsets for both classification approaches.

Data subset	General model	Fantastico model	Femminello model
Training input shape	(5328, 224, 224, 3)	(3168, 224, 224, 3)	(2160, 224, 224, 3)
Training output shape	(5328, 8)	(3168, 9)	(2160, 5)
Validation input shape	(1776, 224, 224, 3)	(1056, 224, 224, 3)	(720, 224, 224, 3)
Validation output shape	(1776, 8)	(1056, 9)	(720, 5)
Test input shape	(1776, 224, 224, 3)	(1056, 224, 224, 3)	(720, 224, 224, 3)
Test output shape	(1776, 8)	(1056, 9)	(720, 5)

3. Results and discussion

The performances of the proposed architectures with those of popular pre-trained CNN architectures using *transfer learning* were compared. These pre-trained architectures achieve high accuracy on extensive specific datasets, such as ImageNet, and we can reuse them with minor modifications for our goal. In the literature, one can find examples where transfer learning models achieve accuracies comparable to custom-built models for various image classification tasks, while generally maintaining lower training times (Kim et al., 2020; Hossain et al., 2018; Shao et al., 2018).

These models were initially trained for different purposes. In all cases, fewer than 100 epochs were sufficient to stop the training using early stopping, with a patience of 10 epochs.

However, one can benefit from the learned features encoded into their weights to build a powerful model for tackling different problems by fine-tuning the last layer or layers of the model. These layers, built and trained from scratch, are usually the *top* layers, the fully connected parts of the model. This implies that the number of parameters required to be tuned is drastically reduced relative to the total number of parameters in the model, thereby saving valuable time during the model training stage.

The classification metrics for the test set (20 % of the samples) for the General, Fantastico, and Femminello models are presented in Tables 7, 8, and 9, respectively.

We observed a consistent advantage of the custom model in all experiments. The second best performer was the VGG-16-based model, followed by the VGG-19-based model and the Xception-based one. Despite being simpler in size and number of parameters than the transfer learning alternatives, the custom model offers the best results in both classification approaches (general and separate models). The most complex models, such as VGG-19 and Xception, are less accurate. One possible reason is that larger models overfit the data, whereas simpler models do not. The fact that VGG-16 performed better than VGG-19 despite being simpler supports this hypothesis. Moreover, the separate models obtained better accuracies than the general model. This suggests that the CNN models can identify differences in the images of different cultivars, which may have unique characteristics and patterns in their images that individual models better capture. A general model may

Table 7
Classification summary for the general model. The best results are highlighted in bold.

Model	Accuracy	Precision	Recall	F1-Score
Custom	0.761	0.766	0.761	0.762
VGG-16 based	0.747	0.760	0.747	0.750
VGG-19 based	0.694	0.718	0.694	0.698
Xception based	0.653	0.642	0.653	0.631

Table 8
Classification summary for Fantastico model. The best results are highlighted in bold.

Model	Accuracy	Precision	Recall	F1-Score
Custom	**0.795**	**0.800**	**0.795**	**0.793**
VGG-16 based	0.782	0.795	0.782	0.780
VGG-19 based	0.772	0.780	0.772	0.771
Xception based	0.739	0.749	0.739	0.736

Table 9
Classification summary for Femminello model. The best results are highlighted in bold.

Model	Accuracy	Precision	Recall	F1-Score
Custom	**0.797**	**0.809**	**0.797**	**0.791**
VGG-16 based	0.788	0.791	0.788	0.784
VGG-19 based	0.753	0.766	0.753	0.745
Xception based	0.664	0.667	0.664	0.661

struggle to discern and accommodate these cultivar-specific nuances.

A confusion matrix is generated for each trained model using the best weights. The results of the General, Fantastico and Femminello models are shown in Figs. 3, 4 and 5, respectively. Part of the error can be explained by the natural variations in the colour of Bergamot. During the ripening process, the chemical composition of fruits can change significantly due to the synthesis and accumulation of specific compounds, including EO. The speed of maturation varies depending on various factors, such as soil or nutrition. In addition, orientation respecting the sun can influence colour evolution from green to yellow. These variations can result in fruits with similar colours having different EO concentrations, confusing the classifiers.

In general, the Xception model performed poorly in all tests. This is because this particular learning problem does not benefit from the depth-wise separable convolutions of this method.

Table 10 summarises the performance results of the General, Fantastico, and Femminello models for the test set. Besides MSE, other metrics have been included: mean absolute error (MAE) and mean absolute percentage error (MAPE).

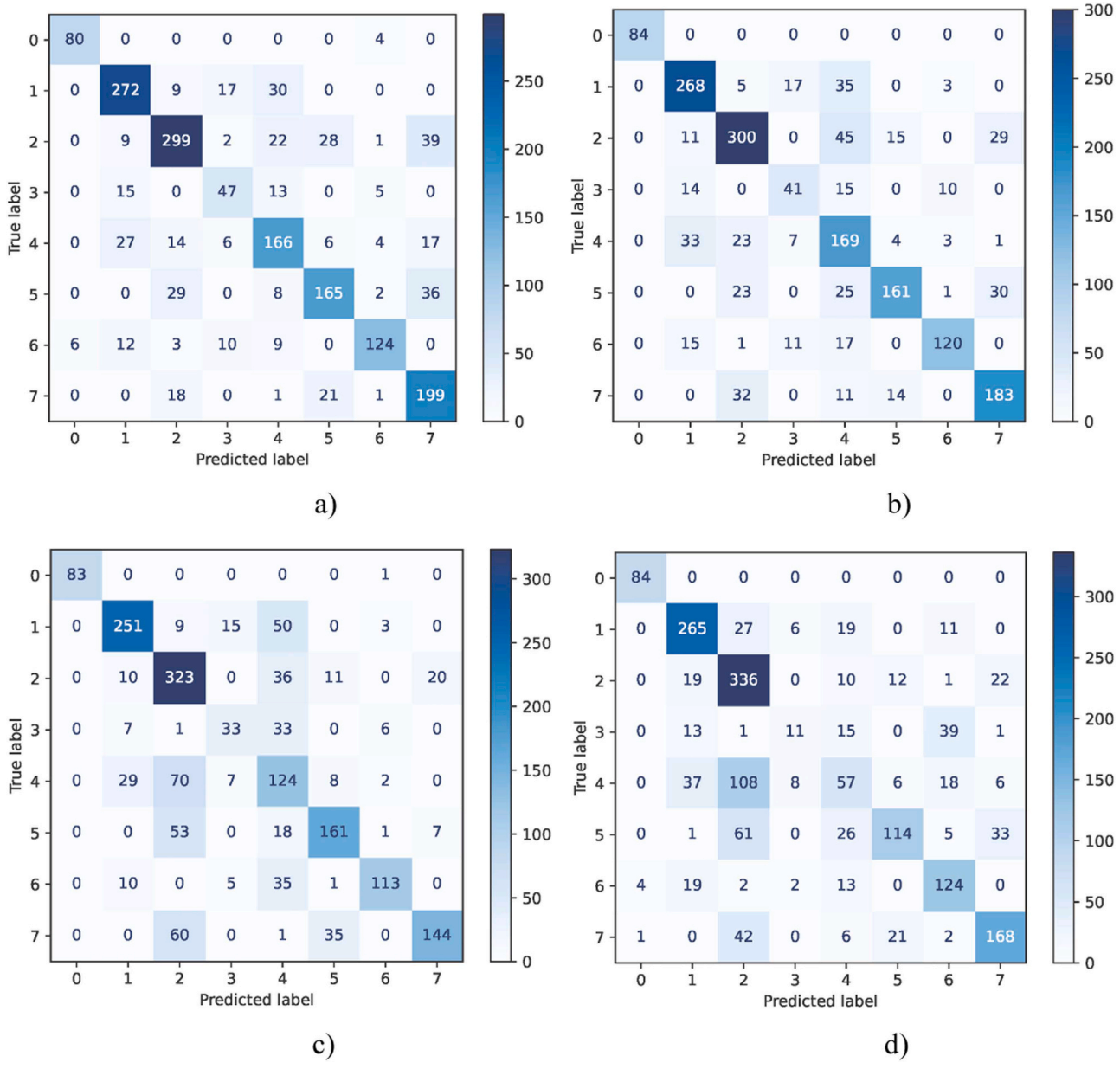

Fig. 3. Confusion matrices for the general model's test set using the different architectures: a) Custom model; b) VGG-16 based; c) VGG-19 based; d) Xception based.

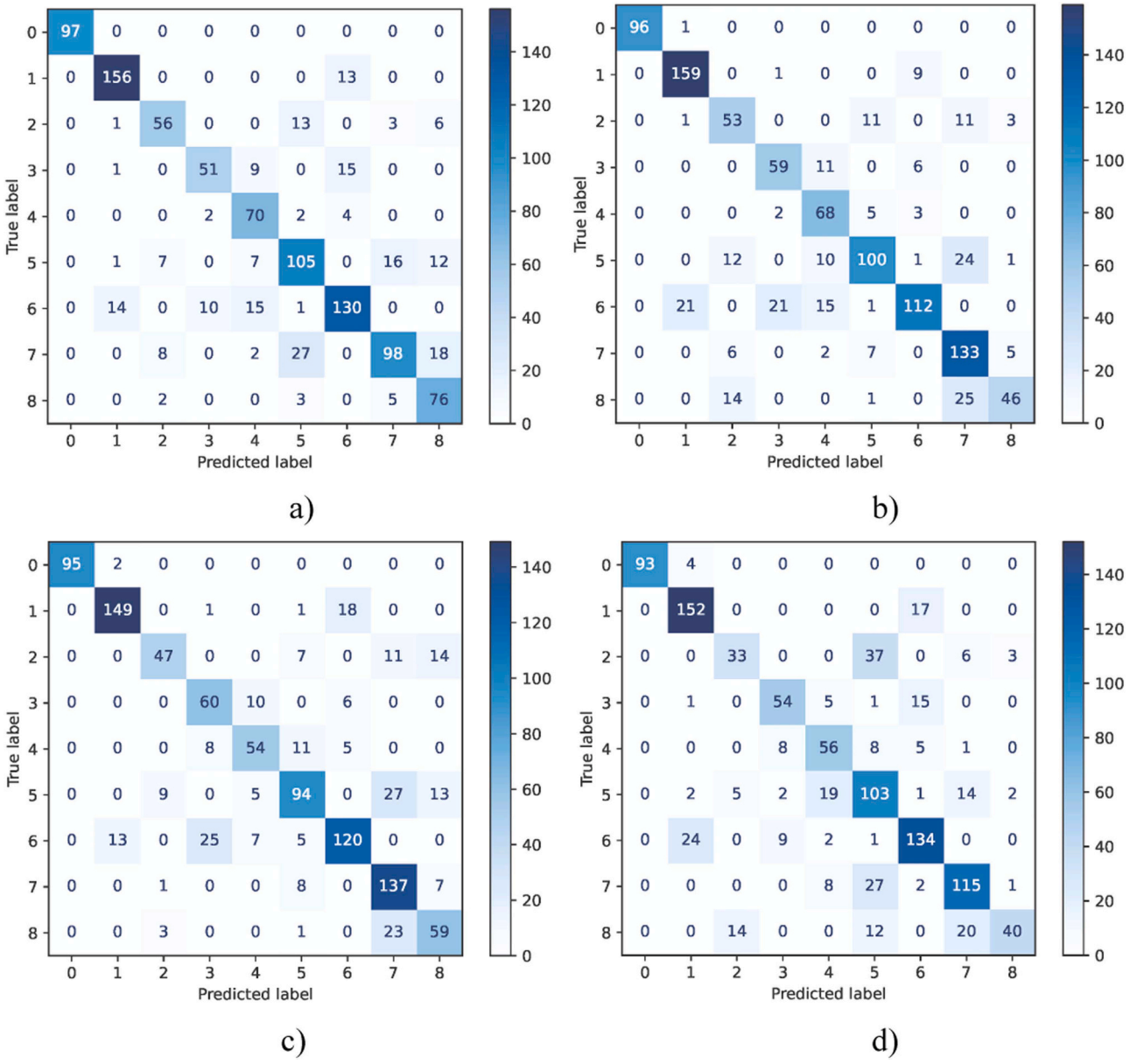

Fig. 4. Confusion matrices for Fantastico test set using the different network architectures: a) Custom model; b) VGG-16 based; c) VGG-19 based; d) Xception based.

The results showed that using separate regression models for the two cultivars was more accurate than using a single model alone. In particular, MSE on the model for cv Femminello was reduced by a factor of 3.2 (> 2 % MAPE improvement), whereas the cv Fantastico obtained roughly the same performance regardless of the approach. The agreement between the results of the classification approach and the performance of separate models in the regression approach further reinforces the idea that modelling each cultivar independently is beneficial.

Concerning BEO, several studies (Dugo and Bonaccorsi, 2013; Verzera et al., 2000; Giuffrè., 2019; Bourgou et al., 2012; Sawamura et al., 2006; Rowshan and Najafian, 2015; Cautela et al., 2021) show that obtaining an annual product with constant values is complex, depending on many factors such as cultivar, ripening stage, climate, the year of production, the age of the plant, agronomic techniques, etc. However, the same in-depth information is unavailable for the oil yield in fruit peels, which also depends on the extraction method. However, no previous studies have established a method for estimating the EO yield in bergamot peel. Hydrodistillation was applied in the present study because it is easy to perform in the laboratory. Other extraction methods, such as supercritical extraction, are expensive in terms of the cost of the apparatus and extractive procedure and are more challenging to manage in a laboratory. Industrial EO extraction involves hundreds of kilos of fruit for each harvest date and cannot be applied in experiments such as the one designed here. The tested CCI values are an acceptable starting point for EO content studies. The study also showed that the amount of EO was higher in cv Fantastico, and the highest level occurred in mid-to-late November. Meanwhile, for cv Femminello, this period was between the beginning and middle of November. Generally, it is possible to observe a gradual and never abrupt transition in the EO content.

According to Ming et al. (2020), smartphone cameras can easily acquire high-quality images directly in the field. A low-cost portable inspection chamber was designed to eliminate the effects of natural light on image capture, optimise data collection from smartphones, create an environment that limits the influence of external factors, and standardise the data collected. This can be a helpful tool for developing new technologies and postharvest operations.

The most recent studies in similar fields were by Dos Santos et al. (2023), who determined eugenol in clove EO using a smartphone, an

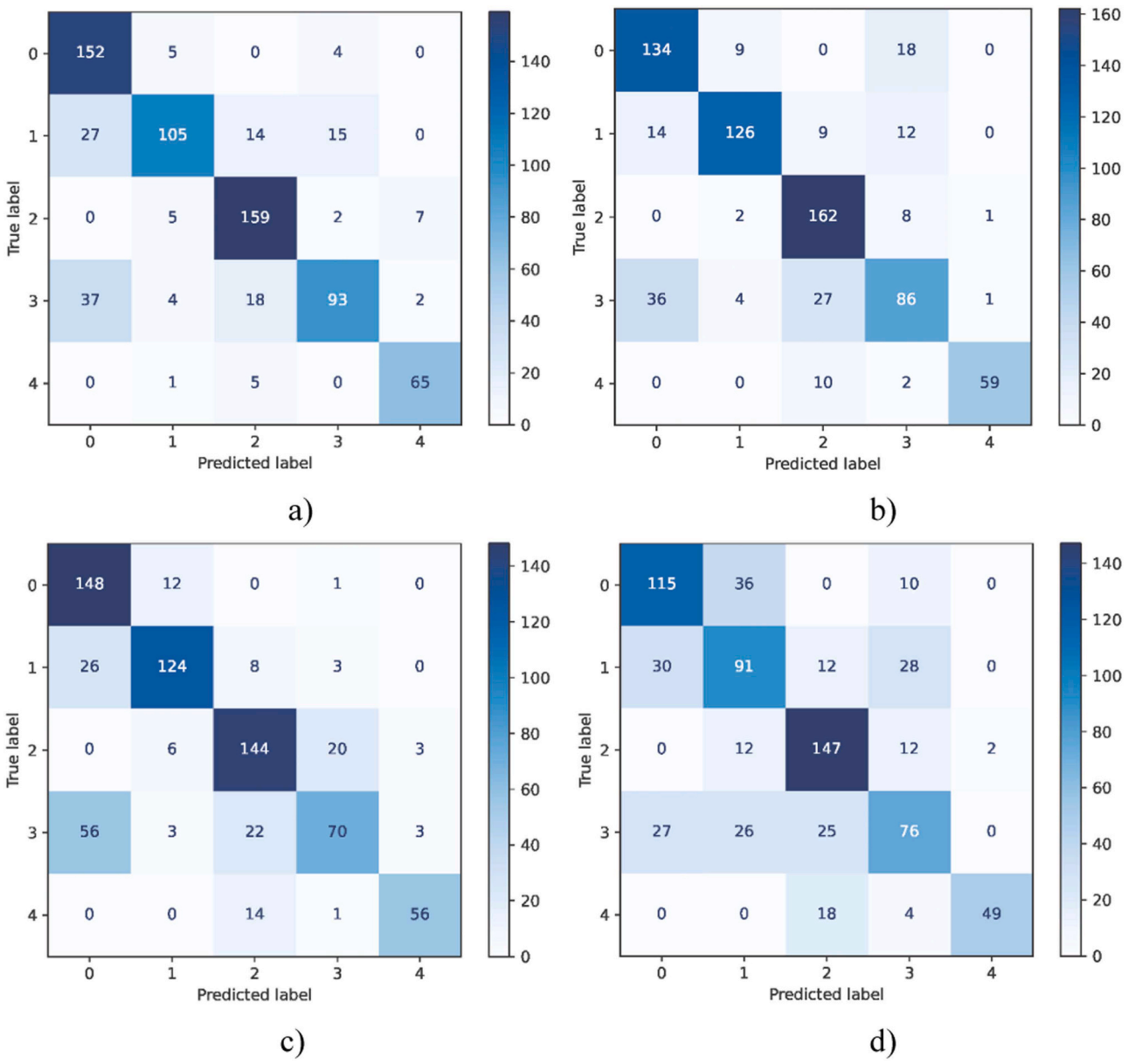

Fig. 5. Confusion matrices for Femminello test set using the different network architectures: a) Custom model; b) VGG-16 based; c) VGG-19 based; d) Xception based.

Table 10
Regression performance summary on the test set.

Metric	General model	Fantastico model	Femminello model
MSE	0.112	0.117	0.035
MAE	0.246	0.257	0.149
MAPE	6.326	6.386	4.024

endoscopic camera, and a 3D printed device, and by Lebanov and Paull (2021), who used a smartphone-based miniaturised Raman spectrometer and machine learning for the rapid identification and discrimination of adulterated EO. Hakonen and Beves (2018) developed a simple method to authenticate edible oils using a 405 nm LED flashlight and a smartphone.

Several studies on the relationship between EO or oil content and fruit ripening have recently been conducted to determine the optimal harvest date. Bourgou et al. (2012) and Bhuyan et al. (2015) studied the variation in EO during citrus peeling and found that it depended on the stage and species. The stage of maximum EO yield was immature for *Citrus limon L.* (Rutaceae), semi-mature for *Citrus sinensis L.* (Rutaceae) and *Citrus reticulata L.* (Rutaceae), and mature for *Citrus aurantium L.* (Rutaceae). Wu et al. (2013) observed a significant increase in EO during fruit development and ripening in *Citrus medica L.* (Rutaceae). Rowshan and Najafian (2015) investigated the effect of the ripening stage on the chemical composition of EO extracted from the peel of bitter orange (*C. aurantium*). The results showed that the ripening stage affected the EO composition. Di Rauso Simeone et al., (2020) showed that the variation of peel EOs during fruit ripening depends on the origin and cultivar of lemons (maximum yield in November for *'Ovale di Sorrento'* and *'Sfusato Amalfitano'* lemons, whereas the peak was reached in December for *'Femminello Cerza'* and *'Femminello Adamo'*). Ghani et al. (2021) studied the EO content of grapefruit peels (*Citrus paradisi L* (Rutaceae) var. red blush) during the colour change stages and found significant changes during the fruit ripening stages.

This can contribute to the introduction of digital technology solutions to improve the agricultural sector's competitiveness and help stakeholders make smart decisions regarding their production processes under a precision agriculture strategy. The challenge is calibrating

learning algorithms to perform well when applied to unknown input data.

4. Conclusions

This study aimed to investigate around EO content of bergamot using a CNN combined with field images captured by a smartphone camera. A custom CNN model trained from scratch and several transfer learning models based on VGG-16, VGG-19, and Xception were fine-tuned using available data. Positive results were obtained with some tested models, achieving accuracies of 0.795 and 0.797 for each cultivar on the test set when using independent models for each cultivar and 0.761 when using a general model for both. Separate regression models were also more capable than one in predicting the EO content. A separate model for cv Femminello enabled an MSE reduction in test samples by a factor of 3.2. The models performed well, which suggests that the method is very robust and can be used to estimate EO, also in different cultivars. Finally, this study has some limitations, mainly related to the impossibility of measuring the essence content of each fruit, one by one, and of taking into account all the agronomic variables related to the site. In addition, mobile phone cameras only operate in the visible spectrum; therefore, developing systems that operate in non-visible absorption bands, such as NIR or SWIR, would certainly improve the accuracy of the results. Moreover, the output of this prediction model can be improved through further research. The long-term goal is to apply it in real-time via mobile phones from the perspective of Agriculture 4.0, which would enable the prediction of bergamot EO content according to fruit colour, with high accuracy, ease of use, and low cost, directly in the field, to support and simplify the hard work of farmers.

CRediT authorship contribution statement

Angelo Maria Giuffrè: Writing – original draft, Formal analysis, Data curation. **Juan Gómez-Sanchis:** Writing – review & editing, Writing – original draft, Supervision, Resources. **Jose Blasco:** Writing – review & editing, Supervision. **Matteo Anello:** Writing – review & editing, Writing – original draft, Investigation, Formal analysis, Data curation. **Bruno Bernardi:** Writing – review & editing, Writing – original draft, Resources, Project administration, Conceptualization. **Fernando Mateo:** Writing – review & editing, Writing – original draft, Software, Formal analysis, Data curation.

Declaration of Competing Interest

The authors declare that they have no known competing financial interests or personal relationships that could have appeared to influence the work reported in this paper.

Data availability

The data that has been used is confidential.

Acknowledgements

This research was funded by the Italian Ministry of University and Research (MUR) in the framework of a doctorate grant funded within the National Operational Program "Research and Innovation 2014-2020, Innovative Doctorates with Industrial Characterisation". PhD course in Agricultural, Food and Forestry Sciences (SAAF) at the University *Mediterranea* of Reggio Calabria (XXXVI cycle).

This research is co-funded by the projects AEI PID2019-107347RR-C33 and GVA-PROMETEO CIPROM/2021/014.

The authors are thankful to "Azienda Agricola Fratelli Foti" and "Azienda Agricola Patea" for providing bergamot fruit free of charge during the whole period of sampling.

Appendix A. Supporting information

Supplementary data associated with this article can be found in the online version at doi:10.1016/j.indcrop.2024.119233.

References

Amato, A., Castellotti, T., Gaudio, F., Gaudio, G., Lovecchio, R., Pupo D'Andrea, M.R., Peluso, R., 2013. L'agricoltura nella Calabria in cifre 2012; INEA–Istituto Nazionale di Economia Agraria: Roma, Italy. ⟨http://dspace.crea.gov.it/handle/inea/742⟩. Accessed May 25, 2022.

Anello, M., Mateo, F., Bernardi, B., Benalia, S., Zimbalatti, G., Blasco, J., Gómez-Sanchis, J. Is it possible to do a reliable assessment of bergamot colour in the field with a smartphone camera? VII International Conference on Safety, Health, and Welfare in Agriculture and Agro-food Systems (Ragusa SHWA). 6 - 9 September 2023 Ragusa Ibla, Italy. "Unpublished results"

Benalia, S., Bernardi, B., Cubero, S., Leuzzi, A., Larizza, M., Blasco, J., 2015. Preliminary trials on Hyperspectral imaging implementation to detect Mycotoxins in dried figs. Chem. Eng. Trans., 44, pp. 157–162. DOI: 10.3303/CET1544027.

Benalia, S., Calogero, V., Anello, M., Zimbalatti, G., Bernardi, B., 2023. Application of computer vision systems for assessing bergamot fruit external features. Adv. Hortic. Sci. 37 (1), 111–116. https://doi.org/10.36253/ahsc-13911.

Bhuyan, N., Barua, P.C., Kalita, P., Saikia, A., 2015. Physico-chemical variation in peel oils of Khasi mandarin (Citrus reticulata Blanco) during ripening. Indian J. Plant. Physiol. 20, 227–231.

Blahnik, V., Schindelbeck, O., 2021. Smartphone imaging technology and its applications. Adv. Opt. Technol. vol. 10 (3), 145–232. https://doi.org/10.1515/aot-2021-0023.

Bourgou, S., Rahali, F.Z., Ourghemmi, I., Saïdani Tounsi, M., Ourghemmi, I., Tounsi, M. S. 2012. Changes of peel essential oil composition of four Tunisian citrus during fruit maturation. Sci. World J.

Carnagie, J.O., Prabowo, A.R., Budiana, E.P., Singgih, I.K., 2022. Essential oil plants image classification using xception model. ISSN 1877-0509 Procedia Comput. Sci. 204, 395–402. https://doi.org/10.1016/j.procs.2022.08.048.

Cautela, D., Pastore, A., Ferrari, G., Laratta, B., D'Onofrio, N., Balestrieri, M.L., Servillo, L., Castaldo, D., 2021. Global warming threatens the world production of bergamot essential oil. ISSN 0926-6690 Ind. Crops Prod. 172, 113986. https://doi.org/10.1016/j.indcrop.2021.113986.

Chollet, F., 2017. Xception: Deep learning with depthwise separable convolutions. In Proceedings of the IEEE conference on computer vision and pattern recognition (pp. 1251-1258).

Cohen, B., Edan, Y., Levi, A., Alchanatis, V., 2022. Early detection of grapevine (Vitis vinifera) downy mildew (Peronospora) and diurnal variations using thermal imaging. Sensors 22, 3585. https://doi.org/10.3390/s22093585.

Consorzio di tutela del bergamotto. http://www.consorziodituteladelbergamotto.it/everything-on-bergamotto/%ef%bf%bca-close-up-look-at-the-legend/the-cultivars-the-use-of-the-fruit-and-its-newly-discovered-health-giving-properties/?lang=en, 2023 (accessed 08.06.23).

Cubero-García, S., Albert Gil, F.E., Prats-Montalbán, J.M., Fernandez-Pacheco, D.G., Blasco Ivars, J., Aleixos Borrás, M.N., 2018. Application for the estimation of the standard citrus colour index (CCI) using image processing in mobile devices. Biosyst. Eng. 167, 63–74. https://doi.org/10.1016/j.biosystemseng.2017.12.012.

Deng, J., et al., 2009. Imagenet: a large-scale hierarchical image database. 2009 IEEE conference on computer vision and pattern recognition 248–255.

Di Donna, L., Bartella, L., De Vero, L., Gullo, M., Giuffrè, A.M., Zappia, C., Capocasale, M., Poiana, M., D'Urso, S., Caridi, A., 2020. Vinegar production from Citrus bergamia by-products and preservation of bioactive compounds. Eur. Food Res. Technol. 246, 1981–1990. https://doi.org/10.1007/s00217-020-03549-1.

Di Rauso Simeone, G., Di Matteo, A., Rao, M.A., Di Vaio, C., 2020. Variations of peel essential oils during fruit ripening in four lemon (Citrus limon (L.) Burm. F.) cultivars. J. Sci. Food Agric. 100, 193–200.

Dos Santos, I.C., Schlesner, S.K., de Moraes, D.P., Fereira, D.F., Voss, M., Giacomelli, S.R., Barin, J.S., 2023. Smartphone-based rapid and low-cost method for the determination of eugenol content of clove essential oil. [Método rápido e de baixo custo empregando smartphone para a determinação de eugenol em óleo essencial de cravo]. Cienc. Rural 53 (10). https://doi.org/10.1590/0103-8478cr20220498.

Dugo, G.; Bonaccorsi, I., 2013. Citrus Bergamia: Bergamot and its Derivatives; CRC Press: Boca Raton, FL, USA, 2013; ISBN 9781439862278.

El-Attar, N.E., Hassan, M.K., Alghamdi, O.A., Award, A.W., 2020. Deep learning model for classification and bioactivity prediction of essential oil-producing plants from Egypt. Sci. Rep. 10, 21349 https://doi.org/10.1038/s41598-020-78449-1.

Elgendy, M., 2020. Deep Learning for Vision Systems. Simon and Schuster, New York, NY, USA.

Fajardo Muñoz, S.E., Freire Castro, A.J., Mejía Garzón, M.I., Páez Fajardo, G.J., Páez Gracia, G.J., 2023. Artificial intelligence models for yield efficiency optimisation, prediction, and production scalability of essential oil extraction processes from citrus fruit exocarps. Front. Chem. Eng. 4, 1055744 https://doi.org/10.3389/fceng.2022.1055744.

Fatta Del Bosco, S.; Abbate, L.; Mercati, F.; Napoli, E.; Ruberto, G., (2020). Essential Oils in Citrus. In The Citrus Genome; Gentile, A., La Malfa, S., Deng, Z., Eds.; Springer International Publishing: Cham, Switzerland, 2020; pp. 211–223. ISBN 9783030153083.

Fazari, A., Pellicer-Valero, O.J., Gómez-Sanchıs, J., Bernardi, B., Cubero, S., Benalia, S., Zimbalatti, G., Blasco, J., 2021. Application of deep convolutional neural networks

for the detection of anthracnose in olives using VIS/NIR hyperspectral images. ISSN 0168-1699 Comput. Electron. Agric. 187, 106252. https://doi.org/10.1016/j.compag.2021.106252.
Ghani, A., Mohtashami, S., Jamalian, S., 2021. Peel essential oil content and constituent variations and antioxidant activity of grapefruit (Citrus × paradisi var. red blush) during color change stages. J. Food Meas. Charact. 15, 4917–4928.
Gioffrè, G., Ursino, D., Labate, M.L.C., Giuffrè, A.M., 2020. The peel essential oil composition of bergamot fruit (Citrus Bergamia, Risso) of Reggio Calabria (Italy): a review. Emir. J. Food Agric. Vol. 32 (11) https://doi.org/10.9755/ejfa.2020.v32.i11.2197.
Giuffrè, A.M., 2019. Bergamot (Citrus bergamia, Risso): The effects of cultivar and harvest date on functional properties of juice and cloudy juice. Antioxidants 8, 221.
Gonzalez-Gonzalez, M.G., Blasco, J., Cubero, S., Chueca, P., 2021. Automated detection of tetranychus urticae koch in citrus leaves based on colour and vis/nir hyperspectral imaging. Agronomy 11 (5), 1002. https://doi.org/10.3390/AGRONOMY1105100.
Hakonen, A., Beves, J.E., 2018. Hue parameter fluorescence identification of edible oils with a smartphone. ACS Sens. 3 (10), 2061–2065. https://doi.org/10.1021/acssensors.8b00409.
Hossain, M.S., Al-Hammadi, M., Muhammad, G., 2018. Automatic fruit classification using deep learning for industrial applications. IEEE Trans. Ind. Inform. 15 (2), 1027–1034.
Hunter, M., 2010. Essential Oils: Art, Agriculture, Science, Industry and Entrepreneurship. Nova Science Publishers, Inc, Hauppauge, NY, USA.
International Organization for Standardization (ISO). Aromatic natural raw materials – Vocabulary. ISO 9235:2013. Published 2014-09-10.
Jia, W., Tian, Y., Luo, R., Zhang, Z., Lian, J., Zheng, Y., 2020. Detection and segmentation of overlapped fruits based on optimised mask R-CNN application in apple harvesting robot. Comput. Electron. Agric. 172 https://doi.org/10.1016/j.compag.2020.105380.
Jiménez-Cuesta, M.J., Cuquerella, J., Martínez-Jávega, J.M., 1981. Determination of a color index for citrus fruit degreening. Proc. Int. Soc. Citric. Vol. 2, 750–753.
Kamilaris, A., Prenafeta-Boldú, F.X., 2018. A review of the use of convolutional neural networks in agriculture. J. Agric. Sci. 156 (3), 312–322. https://doi.org/10.1017/S0021859618000436.
Kim, Y.G., Kim, S., Cho, C.E., Song, I.H., Lee, H.J., Ahn, S., Park, S.Y., Gong, G., Kim, N., 2020. Effectiveness of transfer learning for enhancing tumor classification with a convolutional neural network on frozen sections. Sci. Rep. 10 (1), 1–9.
Kujawa, S., Niedbała, G., 2021. Artificial neural networks in agriculture (MDPI AG). Agriculture 11 (6), 497. https://doi.org/10.3390/agriculture11060497.
Lebanov, L., Paull, B., 2021. Smartphone-based handheld raman spectrometer and machine learning for essential oil quality evaluation. Anal. Methods 13 (36), 4055–4062. https://doi.org/10.1039/d1ay00886b.
Lohar, S., Zhu, L., Young, S., Graf, P., Blanton, M., 2021. Sensing technology survey for obstacle detection in vegetation. Future Transp. 1, 672–685. https://doi.org/10.3390/futuretransp1030036.
Ming, T., Xu, M., Xunan, H., Chuang, L., Ruoling, D., Kaiming, L., Long, Q., 2020. Smartphone-based detection of leaf color levels in rice plants. ISSN 0168-1699 Comput. Electron. Agric. 173, 105431. https://doi.org/10.1016/j.compag.2020.105431.
Munera, S., Rodríguez-Ortega, A., Aleixos, N., Cubero, S., Gómez-Sanchis, J., Blasco, J., 2021. Detection of invisible damages in 'rojo brillante' persimmon fruit at different stages using hyperspectral imaging and chemometrics. Foods 10 (9), 2170. https://doi.org/10.3390/foods10092170.
Navarra, M., Mannucci, C., Delbò, M., Calapai, G., 2015. Citrus bergamia essential oil: from basic research to clinical application. Front. Pharmacol. 6, 36. https://doi.org/10.3389/fphar.2015.00036.
Patrizia Capua (2015), La Repubblica. http://www.repubblica.it/economia/rapporti/impresa-italia/manifattura/2015/03/30/news/profumeria_cosi_il_bergamotto_conquista_le_attenzioni_delle_griffe-110846339/#:~:text=Il%20bergamotto%2C%20all'opposto%20dell,i%2012%2D10%20delle%20arance (accessed 08.06.23).
Paymode, A.S., Malode, V.B., 2022. Transfer learning for multi-crop leaf disease image classification using convolutional neural network VGG. Artif. Intell. Agric. 6, 23–33.
Quirino, A., Giorgi, V., Palma, E., Marascio, N., Morelli, P., Maletta, A., Divenuto, F., De Angelis, G., Tancrè, V., Nucera, S., Gliozzi, M., Musolino, V., Carresi, C., Mollace, V., Liberto, M.C., Matera, G., 2022. Citrus bergamia: kinetics of antimicrobial activity on clinical isolates. Antibiotics 11 (3), 361. https://doi.org/10.3390/antibiotics11030361.
Rowshan, V., Najafian, S., 2015. Changes of peel essential oil composition of Citrus aurantium L. during fruit maturation in Iran. J. Essent. Oil Bear. Plants 18, 1006–1012.
Sawamura, M., Onishi, Y., Ikemoto, J., Thi Minh Tu, N., Thi Lan Phi, N., 2006. Characteristic odour components of bergamot (Citrus bergamia Risso) essential oil. Flavour Fragr. J. 21, 609–615.
Shao, S., McAleer, S., Yan, R., Baldi, P., 2018. Highly accurate machine fault diagnosis using deep transfer learning. IEEE Trans. Ind. Inform. 15 (4), 2446–2455.
Simonyan, K. & Zisserman, A. (2014). Very deep convolutional networks for large-scale image recognition. arXiv preprint arXiv:1409.1556.
Sola-Guirado, R.R., Bayano-Tejero, S., Aragón-Rodríguez, F., Bernardi, B., Benalia, S., Castro-García, S., 2020. A smart system for the automatic evaluation of green olives visual quality in the field. ISSN 0168-1699 Comput. Electron. Agric. 179 (2020), 105858. https://doi.org/10.1016/j.compag.2020.105858.
Teke, M., Deveci, H.S., Haliloğlu, O., Gürbüz, S.Z., Sakarya, U., 2013. A short survey of hyperspectral remote sensing applications in agriculture. In 2013 6th International Conference on Recent Advances in Space Technologies (RAST). IEEE, pp. 171–176 (June).
Verzera, A., La Rosa, G., Zappalà, M., Cotroneo, A., 2000. Essential oil composition of different cultivars of bergamot grown in Sicily. Ital. J. Food Sci. 4, 493–501.
Wang, J., Cao, B., Yu, P., Sun, L., Bao W., Zhu. X., 2018. Deep Learning towards Mobile Applications, 2018 IEEE 38th International Conference on Distributed Computing Systems (ICDCS), 2018, pp. 1385-1393, doi: 10.1109/ICDCS.2018.00139.
Wu, Z., Li, H., Yang, Y., Zhan, Y., Tu, D., 2013. Variation in the components and antioxidant activity of Citrus medica L. var. Sarcodactylis essential oils at different stages of maturity. Ind. Crops Prod. 46, 311–316.